Iterative Image Formation using Fast (Re/Back)-projection for Spotlight-mode SAR

Shaun I. Kelly, Gabriel Rilling, Mike Davies and Bernard Mulgrew
Institute for Digital Communications
The University of Edinburgh
email: {Shaun.Kelly, G.Rilling, Mike.Davies, B.Mulgrew}@ed.ac.uk

***Abstract*— Iterative SAR image formation can visually improve image reconstructions from under-sampled phase histories by approximately solving a regularised least squares problem. For iterative inversion to be computationally feasible, fast algorithms for the observation matrix and its adjoint must be available. We demonstrate how fast, $N^2 \log_2 N$ complexity, (re/back)-projection algorithms can be used as accurate approximations for the observation matrix and its adjoint, without the limiting assumptions of other $N^2 \log_2 N$ methods, e.g. the polar format algorithm. Experimental results demonstrate the effectiveness of iterative methods using a publicly available SAR dataset. `Matlab/C` code implementations of the fast (re/back)-projection algorithms used in this paper have been made available.**

I. Introduction

The data acquisition in a Synthetic Aperture Radar (SAR) system, with some widely accepted assumptions: free space propagation, scalar wavefields, static targets and single bounce scattering of reflectors, can be modelled as a linear system. The discretisation of this linear system is

$$y = \Phi f + n, \tag{1}$$

Where f is the SAR image (represented as a vector), Φ is the system's observation matrix, y is the acquired data (phase history) and n is a noise term which models additive noise sources in the system.

Traditional image formation involves approximating the pseudo inverse $\Phi^\dagger$, using the observation matrix adjoint Φ^H. This leads to the *filtered adjoint* reconstruction which applies a linear filter to the adjoint to make it a close approximation of $\Phi^\dagger$. The filtered adjoint reconstructs good quality images when the phase history is densely sampled. However, if there is missing data or the image is irregularly sampled the visual quality of the reconstruction can deteriorate.

Rather than using a filtered adjoint reconstruction to approximate $\Phi^\dagger$, iterative algorithms can compute $\Phi^\dagger$ by solving the minimum of the least squares (LS)

$$f = \underset{\tilde{f}}{\operatorname{argmin}} \|y - \Phi\tilde{f}\|_2^2, \tag{2}$$

Iterative algorithms using a conjugate gradient give accurate approximations of $\Phi^\dagger$ with a small number of iterations, e.g. LSMR [1]. The computational burden of these algorithms is dominated by a single application of Φ and Φ^H per iteration. Iterative based reconstruction is thus not unreasonable, provided fast implementations of Φ and Φ^H are available. For uniform and densely sampled phase history data, iterative methods only provide minor visual image improvement. However, in a variety of situations it is desirable to produce images from only partial phase history data. Missing data scenarios that can potentially occur in practice include: interruptions along the synthetic appeture, missing frequency bands in the transmitted chirp and strategic under-sampling.

In the missing data scenario equation (2) is ill-posed, therefore regularisation is required to define a unique solution. Regularisation can be added as a penalty to the LS problem as in

$$f = \underset{\tilde{f}}{\operatorname{argmin}} \|y - \Phi\tilde{f}\|_2^2 + \lambda L(\tilde{f}), \tag{3}$$

Where λ is a penalty scalar and L is a penalty function. Typical examples of L are ℓ_p norms, $L(\tilde{f}) = \|\tilde{f}\|_p^p$. $p \leq 1$ has previously been considered for SAR in the context of superresolution [2], [3] and more recently for processing partial SAR data [4], [5]. Other penalty functions such as total variation norms have also been considered for speckle reduction [2]. The use of ℓ_p norms has recently received considerable attention in the context of the emerging field of *compressed sensing* (CS) [6], [7] which theoretically justifies their use (especially in the case $p = 1$) when the SAR image is *compressible*.

Accurate implementations of Φ and Φ^H are commonly referred to as the re-projection algorithm and the back-projection algorithm respectively. Both implementations have a complexity of $\mathcal{O}\left(N^3\right)$, when considering $N \times N$ samples in the phase history and the reconstructed image. In practice a reduced complexity $\mathcal{O}\left(N^2 \log N\right)$ implementation of Φ and Φ^H is commonly used called the Polar Format Algorithm (PFA). The PFA can be implemented very efficiently using nonuniform FFT algorithms [8]. The PFA requires assumptions of constant terrain elevation and flat wavefronts (far-field scenario) which are not required in the (re/back)-projection algorithms. Using techniques from the tomography literature it has been shown that the (re/back)-projection algorithms can also be implemented in $\mathcal{O}\left(N^2 \log N\right)$ operations without the approximations of the PFA [9], [10]. Also, more recently another approach has been shown to provide similar speedup with additional theoretical guarantees regarding the quality of the reconstruction [11]. While still being slower than the PFA,

978-1-4244-8902-2/11/$26.00 ©2011 IEEE

these fast algorithms make it possible to use more accurate Φ and Φ^H in practice resulting in: enhanced image quality and the ability to reconstruct images on non-flat terrain using Digital Elevation Maps (DEM).

II. Synthetic Aperture Radar

A. SAR imaging geometry

In mono-static spotlight-mode SAR, a modulated linear chirp is transmitted and the received signal after it has been dechirped (mixed with a delayed version of the input signal and low-pass filtered) is given by equation (4) (ignoring the Residual Video Phase term) [12].

$$C_\theta(t) = \int_{-L}^{+L} p_\theta(u) \exp\Big\{ -j\frac{2u}{c}(\omega_0 + 2\alpha(t-\tau_0))\Big\} du, \quad (4)$$

for

$$-\frac{T}{2} + \frac{2(R_\theta + L)}{c} \leq t \leq \frac{T}{2} + \frac{2(R_\theta - L)}{c}$$

Where: ω_0 is the carrier frequency, 2α is the chirp rate, T is the chirp duration, L is the radius of the spotlighted region, u is distance in the direction of the transmitted signal with reference to the spotlighted scene centre, $\tau_0 = 2R_\theta/c$, R_θ is the distance to the spotlighted scene centre and $p_\theta(u)$ is the sum of scene reflectivities $f(\overrightarrow{X})$ at a distance $R_\theta + u$ from the antenna and is given by

$$p_\theta(u) = \int_S \delta(\|\overrightarrow{X_\theta} - \overrightarrow{X}\|_2 - (R_\theta + u)) \cdot f(\overrightarrow{X}) dS, \quad (5)$$

Where: $\overrightarrow{X} = (x, y, z(x,y))$ is a point on the scene surface, δ is the Dirac function and $\overrightarrow{X_\theta}$ is the antenna's position for each chirp.

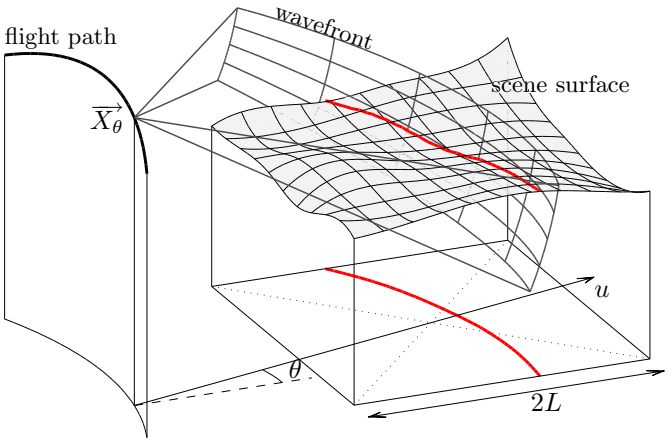

Fig. 1. Data acquisition geometry for spotlight-mode SAR given by equation (4). The red line shows the intersection of the wavefront and the scene surface at a distance $R_\theta + u$ from the antenna. The integral along this line is given by equation (5)

The received signal for each chirp, given by equation (4), is the spatial Fourier transform of the projected scene reflectivities. The discretisation of this equation is the observation matrix Φ.

In equation (5), the altitude of each point of the scene $z(x, y)$ is assumed to be known. This implies that a precise elevation map of the target area is required to implement Φ accurately. Such a precise elevation map is generally not known and only a coarse scale elevation map may be available. In its absence, it is common to assume flat terrain. However, if the scene is not suitably flat, distortion effects and defocussing can results in loss of image resolution [10].

B. SAR image model

In a typical SAR image, most pixels are the result of random sub-pixel interference and a small number are the result of constructive interference. It is therefore convenient to split the image into two parts

$$f = f_s + f_{bg}, \quad (6)$$

With f_s corresponding to the few very bright pixels, resulting from constructive interference, and f_{bg} to the lower reflectivity "background" pixels contaminated by speckle noise, resulting from random interference.

The background pixels contains multiplicative speckle noise and can be modelled as nonstationary complex Gaussian white noise with very high entropy and very low compressibility. This property prevents f_{bg} from being modelled as sparse in any dictionary. Thus precluding the use of CS ideas to recover the full SAR image from an incomplete phase history.

However, the very bright pixels are clearly *sparse* in the image domain and their values are typically much larger than the values in f_{bg}. To recover just f_s, f_{bg} can be treated as noise with a reasonable signal to noise ratio. This suggests that it is possible to use CS to recover f_s, even from a very incomplete phase history.

III. Iterative Image Formation

A. Fast (Re/Back)-projection

The assumption of constant terrain elevation and flat wavefronts is not always valid. If not modeled, spherical wavefronts and topographical variations of the scene's surface can cause blurring and relative distance between objects in the image to be become inaccurate. These effects could also potentially reduce the sparsity of the very bright pixels and thus deteriorate the preformance of CS based reconstructions. Using (re/back)-projection, spherical wavefronts and topographical information in the form of a DEM can be modeled with no additional computational cost.

There has been a number of proposed algorithms for reducing the computational complexity of (re/back)-projection algorithms to $\mathcal{O}\left(N^2 \log_2 N\right)$ in the last decade. These fast algorithms reduce complexity by exploiting redundancy in Φ and Φ^H, e.g. [13] and [9]. In our framework we have used

the latter algorithm which exploits the redundancy through a *divide and conquer* approach.

Range and cross-range sampling periods are linearly proportional to the scene size for constant range and cross-range resolutions [14]. This property lends itself to a divide and conquer strategy where the original scene is recursively split into smaller sub-scenes in a quadtree structure. For simplicity, we will describe the fast re-projection algorithm, the implementation of the fast back-projection is similarly straightforward.

Using the quadtree structure, standard re-projection is performed on all of the small sub-images at their required sampling rate, which is much less than that of the full scene. The phase histories can then be recursively combined up the quadtree, using low-pass upsampling, to produce a single phase history for the whole scene. The approximation errors due to the low-pass upsampling can be managed by choosing appropriate filter lengths. If the original scene is split into sub-scenes of just one sample, the computational complexity of the algorithm becomes $\mathcal{O}\left(N^2 \log_2 N\right)$.

Critically, the fast (re/back)-projection algorithms approach the same complexity as other fast methods without being compromised by the same geometric assumptions. The implementation of the fast re-projection algorithm used in our framework combines four phase-histories at each stage of the recursion with the following steps:

1) 2D low-pass upsample the sub-scene phase histories by a factor of two in range and cross-range using fast filtering in the Fourier domain
2) modify the upsampled phase histories' scene centres $\overrightarrow{X_c}'$ to a combined scene center $\overrightarrow{X_c}$ by multiplying the phase histories by $\exp\Big\{-j\frac{2}{c}(\omega_0+2\alpha(t-\tau_0))(\|\overrightarrow{X_c}'-\overrightarrow{X_\theta}\|_2 - \|\overrightarrow{X_c}-\overrightarrow{X_\theta}\|_2)\Big\}$
3) sum sets of four upsampled phase histories

In a practical implementations the recursion will not continue down to the single pixel stage. This is because the computational requirements of upsampling the phase histories when the sub-scenes are small becomes more computationally expensive than the two times speed up achieved at each stage of recursion.

In our implementation of the fast (re/back)-projection algorithms the recursive (up/down)-sampling stages of the algorithms were implemented in `Matlab` code. For the standard (re/back)-projection a `C` code implementation was used. In our fast algorithms we used $\log_2 N - 6$ levels of recursion. It was found that for higher levels of recursion, computation times started to increase. If the recursive (up/down)-sampling stage was also implemented in `C` code, reduced computation times would be expected for higher levels of recursion. The implementations of the standard and fast (re/back)-projection algorithms are available [15].

To demonstrate the compuational advantages of fast back-projection, Table I shows image formation times for $N \times N$ scenes and phase histories using: standard back-projection (BP), fast back-projection (Fast BP) and a non-uniform FFT implementation of the PFA (written in `C` code).

Figure 2 shows a reconstructed image using the fast back-projection algorithm from 4° of the Gotcha data set [16]. The Gotcha data set is a publicly available collection of phase histories of a 100m $\times$ 100m scene containing both coherent and non-coherent reflectors. Images reconstructed using standard back-projection and fast back-projection are virtually indistinguishable.

TABLE I
IMAGE FORMATION TIMES (SECONDS)

N	BP	Fast BP	PFA
256	2.50	1.06	0.11
512	20.01	5.08	0.60
1024	157.32	24.87	5.55
2048	1254.48	118.69	38.19

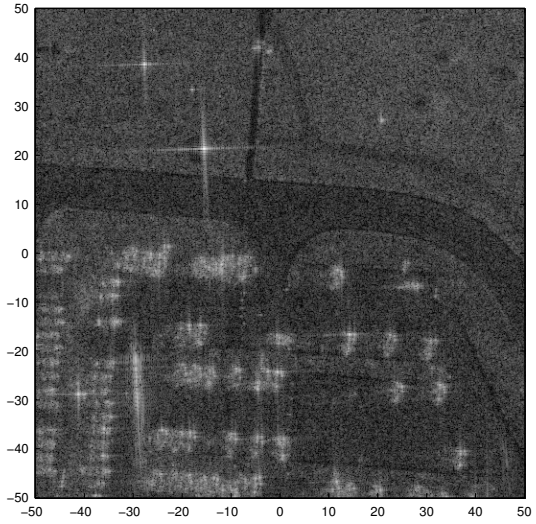

Fig. 2. Fast back-projection reconstruction using 4° of the Gotcha data set.

B. Compressed Sensing SAR

CS theory states that a compressible signal can be well approximated from a significantly reduced number of samples compared to that which is required by the Nyquist-Shannon sampling theorem.

An under-sampled linear system Φ is under-determined and from a traditional sampling perspective its inverse is ill-posed. However, if the vector to be recovered f is known to be approximately sparse under certain conditions it can be accurately approximated by solving the non-linear program (7) [17].

$$f = \arg\min_{\tilde{f}} \|\tilde{f}\|_1 \text{ subject to } \|y - \Phi\tilde{f}\| \leq \epsilon, \qquad (7)$$

Where, ϵ is a small constant which allows for additive noise.

For the noiseless case, i.e. $\epsilon = 0$, it has been shown in [18] that by using the partial Fourier matrix for Φ, equation (7) becomes equivalent to the sparse reconstruction problem

with high probability. The partial Fourier matrix is a random m row subset of the $n \times n$ discrete Fourier matrix. The Φ matrix in randomly under-sampled SAR (the under-sampled re-projection matrix), through the Fourier slice theorem, is analogous to the partial Fourier matrix. The reconstruction of the very bright pixels f_s in a SAR image lends itself to the CS-framework because the features we are trying to reconstruct are sparse.

Using the CS framework, f_s can be reconstructed by equation (8).

$$f_s = \arg\min_{\tilde{f}} \|y - \Phi\tilde{f}\|_2^2 + \lambda\|\tilde{f}\|_1, \tag{8}$$

Where λ is a constant which controls the level of sparsity in the reconstructed image. Fast iterative algorithms exist for equation (8), e.g. GPSR [19]. Like the standard LS algorithms, the computational burden is dominated by a single application of Φ and Φ^H at each iteration. Equation (8) has also been used for fully-sampled data in the context of superresolution [2], [3] due to its sharpening effect on the very bright pixels.

Since sparsity does not benefit the reconstruction of the background, we have to consider using non-sparsity based techniques. A simple way to make the inversion well-posed is to use an ℓ_2 regularisation function. f_{bg} can then reconstructed by

$$f_{bg} = \arg\min_{\tilde{f}} \|y_r - \Phi\tilde{f}\|_2^2 + \lambda\|\tilde{f}\|_2, \tag{9}$$

Where, $y_r = y - \Phi f_s$ is the phase history with the very bright pixels removed. For the optimal λ this problem is equivalent to the pseudo inverse. The pseudo inverse amounts to assuming that the missing data are zeros, so the reconstructed f_{bg} still suffers from poor contrast and high speckle. However, The background pixels in the combined image f have improved image quality when compared to the standard reconstruction methods. This is because in standard methods, the energy from the very bright pixels is spread over the entire image, dominating the low energy background pixels.

Figure 4 demonstrates the visual improvement provided by the mixed ℓ_1 and ℓ_2 regularised LS reconstruction when compared to the filtered back-projection reconstruction. Figures 4(a), 4(c) and 4(e) show filtered back-projection reconstructions, with 75%, 50% and 25% of the full phase history data. Figures 4(b), 4(d) and 4(f) show mixed ℓ_1 and ℓ_2 regularised LS reconstructions of f using 10 iterations of GPSR for f_s and 10 iterations of LSMR for f_{bg}, with 75%, 50% and 25% of the full phase history data. As expected, the visual improvement in f_s, achieved by using a mixed ℓ_1 and ℓ_2 regularised LS reconstruction, is substantial. Reasonable reconstructions of f_s are possible, even in a heavily under-sampled scenario. While, the visual improvement in f_{bg} is more modest. f_{bg} degrades significantly as the level of under-sampling increases.

C. Auto-focus

An error τ_e in the scene centre round trip propagation delay estimate introduces an unknown phase error for each projection. Phase errors can degrade and produce distortions in the reconstructed image. [20]. The phase error for a given τ_e is given by

$$P_{\tau_e}(t) = \exp\Big\{ -j(\omega_o\tau_e + \alpha\tau_e^2) - j2\alpha(t - \tau_o)\Big\}, \tag{10}$$

The phase error consists of a constant phase error $-\omega_o\tau_e - \alpha\tau_e^2$ and a linear phase error $-2\alpha(t - \tau_o)$. The linear phase term produces a radial shift of $\tau_e c/2$ in the range compressed phase history. If a SAR system's timing uncertainty is much less than the reciprocal of the chirp bandwidth $\tau_e \ll 1/B$, the linear phase term can be ignored [20].

Considering just the constant unknown phase error, classical auto-focus methods, such as the Phase Gradient Autofocus (PGA) method [21], indirectly use sparsity to correct phase errors. Using an iterative framework, sparsity can be directly used to correct phase errors by adding them into the reconstruction formulation, as in the following equation

$$(\phi, f_s) = \arg\min_{\tilde{\phi},\tilde{f}} \|y - \Psi(\tilde{\phi})\Phi\tilde{f}\|_2^2 + \lambda\|\tilde{f}\|_1, \tag{11}$$

Where, $\tilde{\phi} \in [-\pi, \pi]^m$ is a vector containing the estimated phase errors and Ψ is a diagonal matrix containing the elements $e^{j\tilde{\phi}}$. Equation 11 aims to concurrently solve the sparse image formation problem and the auto-focus problem. In [22] a very similar approach is demonstrated on fully-sampled synthetic data and images that contain only very bright pixels.

Figure 3(a) and 3(b) shows reconstructions of the same 50% sub-sampled phase history with random phase errors. Figure 3(a) was reconstructed using the mixed ℓ_1 and ℓ_2 regularised LS reconstruction *without* auto-focus. While, figure 3(b) was reconstructed using the mixed ℓ_1 and ℓ_2 regularised LS reconstruction *with* auto-focus.

IV. Conclusion

In this paper we have demonstrated iterative SAR image formation, utilising fast (re/back)-projection algorithms. Accurate iterative reconstructions can be achieved in a small number of iterations, making these type of reconstruction methods not computationally unrealistic. Recent interest in parallel implementations of fast (re/back)-projection algorithms will further increase their feasibility [23]. Iterative reconstructions from under-sampled data showed visual improvements when compared to standard methods. The very bright pixels were recoverable even from heavily under-sampled data. However, background pixel reconstruction from under-sampled data was limited. In some imaging scenarios, iterative SAR image formation utilising fast (re/back)-projection algorithms could be used to provide improved image reconstructions.

V. Acknowledgements

This work was supported in part by: EPSRC grants [EP/F039697/1, EP/H012370/1], the MOD University Defence Research Centre on Signal Processing and the European Commission through the SMALL project under FET-Open, grant number 225913.

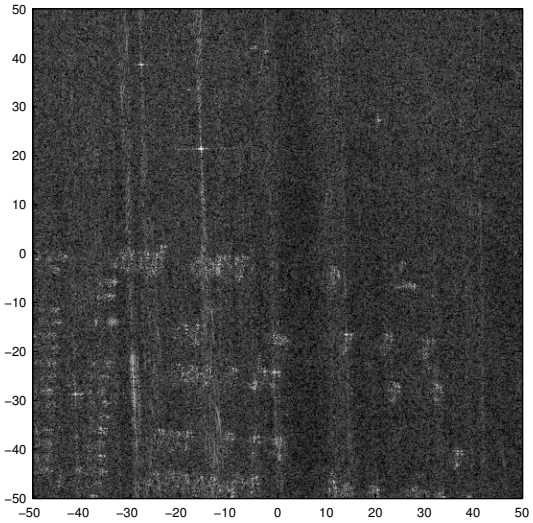

(a)

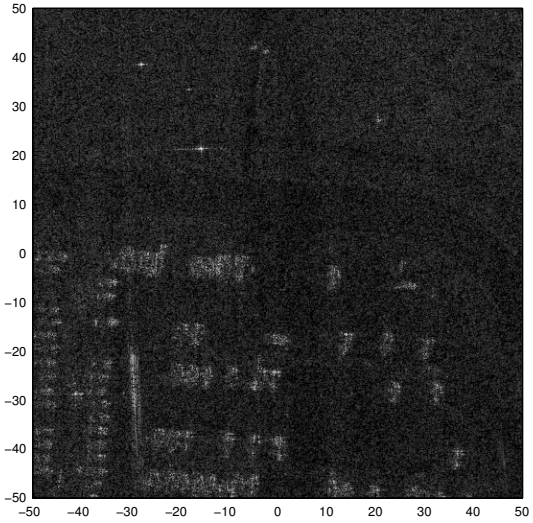

(b)

Fig. 3. Image formation using 4° of the Gotcha data set with phase errors. (a) Mixed ℓ_1 and ℓ_2 regularised LS without auto-focus. (b) Mixed ℓ_1 and ℓ_2 regularised LS reconstruction with auto-focus.

REFERENCES

[1] D. C.-L. Fong and M. A. Saunders, "LSMR: an iterative algorithm for sparse least-squares problems," June 2010. [Online]. Available: http://arxiv.org/abs/1006.0758

[2] M. Çetin, "Feature-enhanced synthetic aperture radar imaging," Ph.D. dissertation, Boston University, 2001.

[3] M. Ferrara, J. Jackson, and C. Austin, "Enhancement of multi-pass 3d circular SAR images using sparse reconstruction techniques," in *Proceedings of SPIE Algorithms for Synthetic Aperture Radar Imagery XVI*, 2009.

[4] M. Çetin and R. L. Moses, "Synthetic aperture radar imaging from wide-angle data with frequency-band omissions," in *IEEE 14th Signal Process. and Commun, App.*, 17-19 2006, pp. 1 –4.

[5] G. Rilling, C. Du, M. E. Davies, and M. Bernard, "Processing SAR data with gaps in the aperture: A compressed sensing perspective," in *Proceedings of International Conference on Synthetic Aperture Sonar and Synthetic Aperture Radar*, September 2010.

[6] E. J. Candes, J. Romberg, and T. Tao, "Robust uncertainty principles: exact signal reconstruction from highly incomplete frequency information," *IEEE Trans. Inf. Theory*, vol. 52, no. 2, pp. 489 – 509, Feb. 2006.

[7] D. L. Donoho, "Compressed sensing," vol. 52, no. 4, pp. 1289–1306, 2006.

[8] L. Greengard and J.-Y. Lee, "Accelerating the nonuniform fast Fourier transform," *SIAM Review*, vol. 46, no. 3, pp. 443–454, 2004.

[9] S. Xiao, D. Munson, S. Basu, and Y. Bresler, "An N^2logN Back-Projection Algorithm for SAR Image Formation," in *Asilomar Conference on Signals Systems and Computers*, vol. 1, 2000, pp. 3–7.

[10] D. Wahl, D. Yocky, and C. Jakowatz Jr, "An implementation of a fast backprojection image formation algorithm for spotlight-mode SAR," in *Proceedings of SPIE Algorithms for Synthetic Aperture Radar Imagery XV*, vol. 6970, 2008, p. 69700H.

[11] L. Demanet, M. Ferrara, N. Maxwell, J. Poulson, and L. Ying, "A butterfly algorithm for synthetic aperture radar imaging," (submitted).

[12] D. Munson Jr, J. O'brien, and W. Jenkins, "A Tomographic Formulation of Spotlight-Mode Synthetic Aperture Radar," *Proceedings of the IEEE*, vol. 71, no. 8, pp. 917–925, 1983.

[13] L. Ulander, H. Hellsten, and G. Stenstrom, "Synthetic-aperture radar processing using fast factorized back-projection," *Aerospace and Electronic Systems, IEEE Transactions on*, vol. 39, no. 3, pp. 760–776, 2003.

[14] W. Carrara, R. Goodman, and R. Majewski, *Spotlight Synthetic Aperture Radar - Signal Processing Algorithms*. Artech House, 1995.

[15] [Online]. Available: http://www.see.ed.ac.uk/~s0977884

[16] C. H. Casteel Jr, L. A. Gorham, M. J. Minardi, S. M. Scarborough, K. D. Naidu, and U. K. Majumder, "A challenge problem for 2D/3D imaging of targets from a volumetric data set in an urban environment," in *Proceedings of SPIE Algorithms for Synthetic Aperture Radar Imagery XIV*, 2007.

[17] E. Candès, J. Romberg, and T. Tao, "Robust uncertainty principles: Exact signal reconstruction from highly incomplete frequency information," *Information Theory, IEEE Transactions on*, vol. 52, no. 2, pp. 489–509, 2006.

[18] M. Rudelson and R. Vershynin, "On sparse reconstruction from Fourier and Gaussian measurements," *Communications on Pure and Applied Mathematics*, vol. 61, no. 8, pp. 1025–1045, 2008.

[19] M. Figueiredo, R. Nowak, and S. Wright, "Gradient projection for sparse reconstruction: Application to compressed sensing and other inverse problems," *Selected Topics in Signal Processing, IEEE Journal of*, vol. 1, no. 4, pp. 586–597, 2008.

[20] C. Jakowatz, D. Wahl, P. Eichel, G. D.C., and P. Thompson, *Spotlight-mode synthetic aperture radar: a signal processing approach*. Kluwer Academic Pub, 1996.

[21] D. Wahl, P. Eichel, D. Ghiglia, and C. Jakowatz Jr, "Phase gradient autofocus-a robust tool for high resolution SAR phase correction," *Aerospace and Electronic Systems, IEEE Transactions on*, vol. 30, no. 3, pp. 827–835, 2002.

[22] N. Önhon and M. Çetin, "A nonquadratic regularization-based technique for joint SAR imaging and model error correction," in *Proceedings of SPIE Algorithms for Synthetic Aperture Radar Imagery XVI*, vol. 7337, 2009, p. 73370C.

[23] A. Rogan and R. Carande, "Improving the fast back projection algorithm through massive parallelizations," in *Proceedings of SPIE Radar Sensor Technology XIV*, vol. 7669, 2010, p. 76690I.

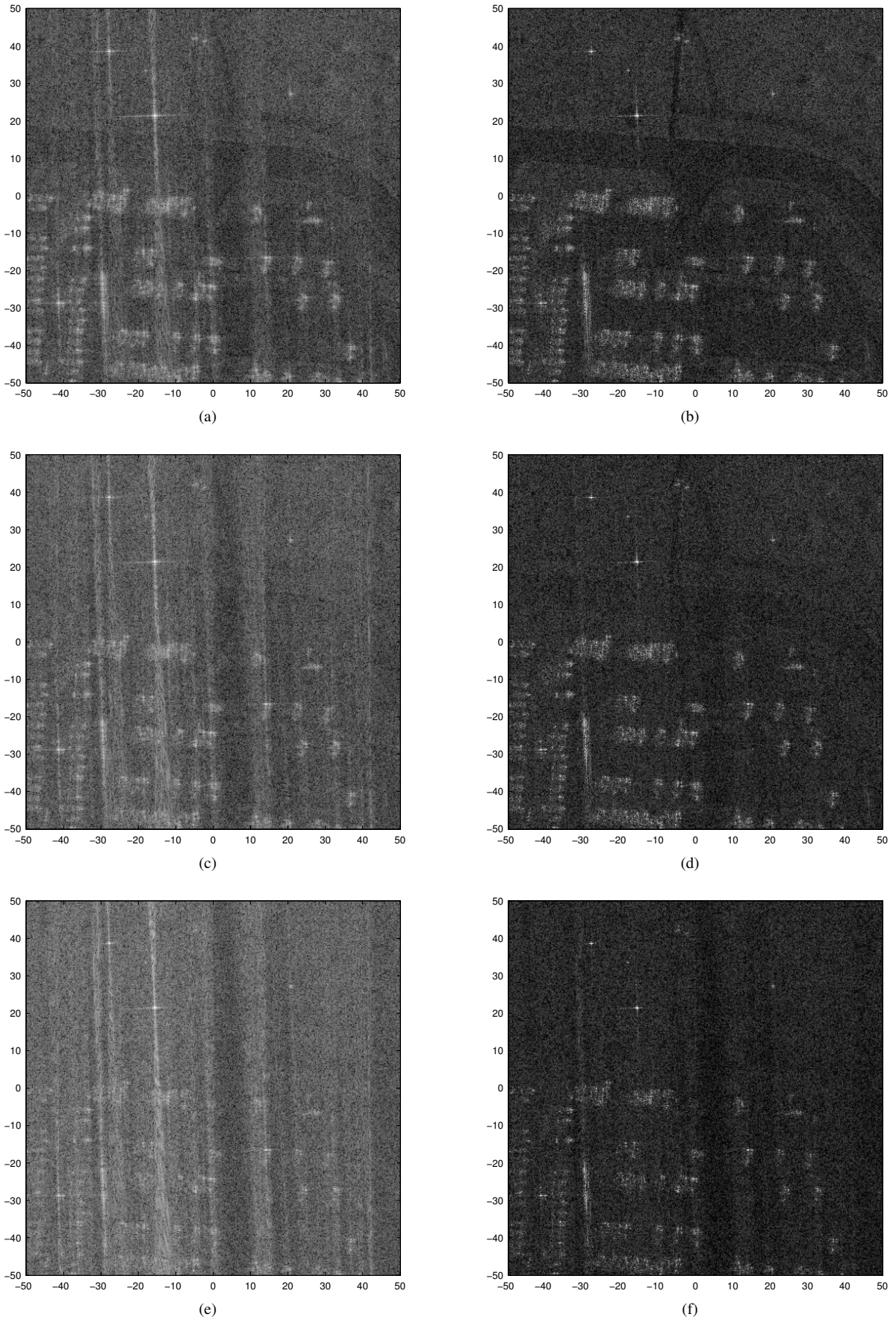

Fig. 4. Image formation using 4° of the Gotcha data set with the phase history uniform randomly under-sampled in cross-range. (a) filtered back-projection reconstruction (75% of full data). (b) mixed ℓ_1 and ℓ_2 regularised LS reconstruction (75% of full data). (c) filtered back-projection reconstruction (50% of full data). (d) mixed ℓ_1 and ℓ_2 regularised LS reconstruction (50% of full data). (e) filtered back-projection reconstruction (25% of full data). (f) mixed ℓ_1 and ℓ_2 regularised LS reconstruction (25% of full data).

978-1-4244-8902-2/11/$26.00 ©2011 IEEE